



HAL
open science

Nested ADMM for PET reconstruction with two constraints: Deep Image Prior and non-negativity in projection space

Alexandre Merasli, Tie Liu, Thomas Carlier, Diana Mateus, Maël Millardet, Saïd Moussaoui, Simon Stute

► To cite this version:

Alexandre Merasli, Tie Liu, Thomas Carlier, Diana Mateus, Maël Millardet, et al.. Nested ADMM for PET reconstruction with two constraints: Deep Image Prior and non-negativity in projection space. 2022 IEEE Nuclear Science Symposium, Medical Imaging Conference and Room Temperature Semiconductor Detector Conference, Nov 2022, Milan, Italy. 10.1109/NSS/MIC44845.2022.10398975 . hal-03930288

HAL Id: hal-03930288

<https://hal.science/hal-03930288>

Submitted on 25 Apr 2024

HAL is a multi-disciplinary open access archive for the deposit and dissemination of scientific research documents, whether they are published or not. The documents may come from teaching and research institutions in France or abroad, or from public or private research centers.

L'archive ouverte pluridisciplinaire **HAL**, est destinée au dépôt et à la diffusion de documents scientifiques de niveau recherche, publiés ou non, émanant des établissements d'enseignement et de recherche français ou étrangers, des laboratoires publics ou privés.

Nested ADMM for PET Reconstruction with Two Constraints: Deep Image Prior and Non-Negativity in Projection Space

Alexandre Merasli, Tie Liu, Thomas Carlier, Diana Mateus, Maël Millardet, Saïd Moussaoui, Simon Stute

Abstract—Radioembolization with ^{90}Y -microspheres is used as a treatment for non-resectable liver cancer. ^{90}Y is mainly a β^- -emitter but a few β^+ particles are also emitted. It enables to quantify the amount of radioactivity in the body using PET imaging, which could be especially useful for dosimetry purpose. Yet, the reconstructed images are very noisy due to the limited amount of collected data with ^{90}Y , and the usual reconstruction algorithms have positive bias in regions with low activity. In this context, we propose to combine two complementary approaches recently published, both using the Alternating Direction Method of Multipliers (ADMM) algorithm, within a nested ADMM. The first one allows for negative values in the image by enforcing the non-negativity in the projection space only, hence reducing the bias. The second one intends to lower the noise in the image by adding the constraint that the reconstructed image is the output of a Deep Image Prior (DIP) network.

I. METHODS

PET data y are modelled as a sample of a Poisson distribution of mean $\bar{y} = Ax + \bar{b}$, where x is the image, A is the system matrix modelling the PET system acquisition and \bar{b} is an additive background (random and scatter coincidences). We want to reconstruct the image by minimizing the negative log-likelihood as in usual PET reconstruction algorithms but adding two constraints:

- The reconstructed image x is the output of the DIP network $f(\theta|z)$ (z being the network input and θ the network weights), as proposed in [3]. The network has a U-Net architecture, with an encoder and a decoder part to denoise the labeled image. The input image z can be random noise, or a prior information like the attenuation μ -map (used in preprocessing steps of the reconstruction to correct for the attenuation effect) or any anatomical image (CT or MR) for real data. The last ReLU layer was removed from the architecture in [3] to not impose positivity on the image.
- The non-negativity is enforced in the projection space ($\bar{y} \geq 0$) while x can be negative, as proposed in [5].

To solve this optimization problem, we adapted the ADMM algorithm in [3] (called ADMMLim here) to deal with the

A. Merasli is with SIEMENS Healthineers, 93210 Saint-Denis, France, and CRCI2NA, INSERM UMR 1307, Nantes, France and Nuclear Medicine Department, University Hospital, Nantes, France (e-mail: alexandre.merasli@univ-nantes.fr).

T. Carlier and S. Stute (so were T. Liu and M. Millardet) are with CRCI2NA, INSERM UMR 1307, Nantes, France and Nuclear Medicine Department, University Hospital, Nantes, France.

D. Mateus and S. Moussaoui (so was M. Millardet) are with Nantes Université, École centrale de Nantes, CNRS, UMR 6004, LS2N, Nantes, France.

network constraint, with the idea of a barrier function g to replace the non-negativity constraint as in [5]. Figure 1 shows the resulting nested ADMM algorithm.

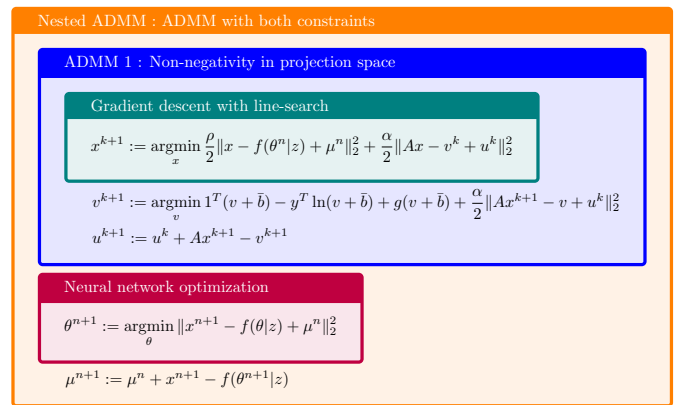


Fig. 1: Complete scheme of the proposed nested algorithm where each block is an iterative algorithm and α and ρ are the ADMM hyper-parameters. The output of the network f after a given number of iterations is taken as the final image.

The nested ADMM algorithm requires several hyperparameters to be tuned. The following two hyperparameters were automatically updated:

- The penalty strength α coming from the first derived ADMM (the blue box in Fig. 1.) was tuned with residual balancing using relative residuals instead of more classical residuals, as suggested in [12].
- The DIP requires to be stopped before convergence to avoid overfitting the noise [10]. Therefore, we used the Window Moving Variance [11] early stopping method for the initialization denoising task of the DIP before the nested ADMM process.

The other hyperparameters were manually tuned, inspired by the tuning in [3].

The deep learning step of the algorithm was done with the Pytorch library, and the reconstruction step was implemented within the CASToR [6] reconstruction framework.

II. EXPERIMENTS

We used 2D analytical simulations [9] of a cylindrical phantom filled with ^{90}Y , including a cold region and a hot region with 5:1 contrast (Fig. 2). 1.5M prompt coincidences were simulated with 90% random fraction and 30% scatter

fraction. Activity recovery was measured in the cold and hot regions and plotted against the image roughness (standard-deviation of pixel values in the background region).

We compared our algorithm to:

- the DIPrecon algorithm [3] which also uses a DIP network inside the reconstruction,
- ADMMLim [5] and APPGML [7] which are algorithms designed to reduce the positive bias in cold regions,
- BSREM [1] and OSEM [4] used in clinical routines.

One hundred statistical replicates of the simulations were reconstructed. DIPRecon and nested ADMM were initialized with a DIP-denoised BSREM as shown in Fig. 2, with standardization scaling, for respectively 100 and 300 iterations. The number of iterations used for ADMMLim was chosen to reach the convergence [12]. APPGML was run for 15 iterations and 28 subsets, with a value of shift A equal to the phantom background. These two algorithms used a Markov Random Field (MRF) quadratic penalty. BSREM was used as in clinics [2], with 30 iterations and 28 subsets and Relative Difference Penalty. These three algorithms were run with different values of penalty strength. OSEM was run for 36 iterations and 28 subsets. Different full-width half-maximum (FWHM) Gaussian filtering were used.

III. RESULTS

Fig. 2 depicts the simulated phantom and an image reconstructed with the current BSREM method available in clinics [2]. Fig. 3 presents images obtained for three methods : the DIPrecon and the proposed algorithms both with hyperparameters tuning as previously explained, and a DIP-denoised BSREM (same settings as in Fig. 2. for BSREM, and without the last ReLU layer for the DIP). Images are shown for one statistical replicate and with average and standard deviation over replicates. Fig. 4 shows trade-off curves of bias and image roughness for all compared algorithms, in the cold and hot regions, for one hundred replicates.

First, in Fig. 3, the cold region is qualitatively whiter for the nested ADMM compared to the DIPrecon. This is expected as the main difference between the two algorithms is the non-negativity constraint in projection space, intending to reduce positive bias in cold regions for the proposed algorithm. Then, we can also see the difference between including the DIP into the reconstruction instead of only using it as a post processing step: the phantom is more clearly defined and less blurry.

Second, in Fig. 4, the nested ADMM algorithm achieves interesting quantitative performance in the hot region, with a high activity recovery for a low amount of noise, even if BSREM can achieve higher activity recovery for a reasonable amount of noise. Then, in the cold region, APPGML and ADMMLim have a small negative bias, whereas DIPrecon and algorithms used in clinics have a positive bias. As for the proposed algorithm, it has low positive bias in the cold region.

IV. DISCUSSION AND PERSPECTIVES

We developed and implemented a new reconstruction method aiming at reducing bias in cold region as well as reducing the image noise thanks to the Deep Image Prior. We used Window Moving Variance and relative residual balancing

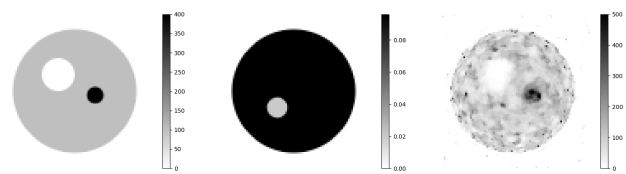


Fig. 2: *Left and middle:* 2D simulated emission and attenuation images. *Right:* image reconstructed using the BSREM algorithm [1] with the relative difference penalty (RDP) [8] as in clinics [2]

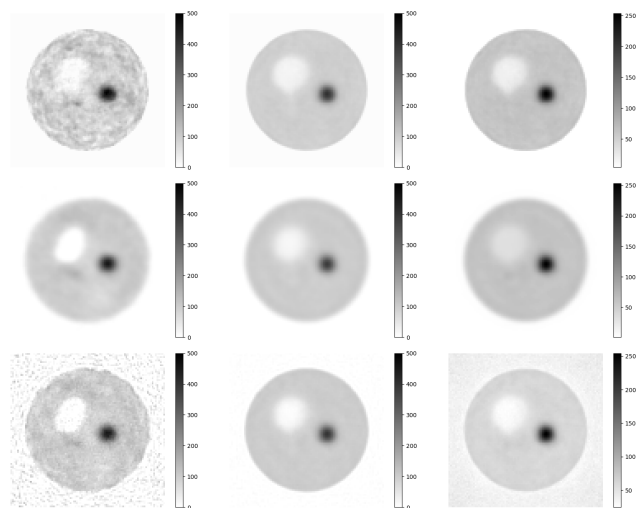


Fig. 3: Comparison between the DIPrecon and the proposed algorithm. For each column, *left:* image for 1 replicate, *middle:* averaged over 100 replicates, *right:* standard deviation over 100 replicates. For each row: *top:* DIPrecon image after 100 global iterations, *middle:* BSREM image denoised by the DIP without ReLU, *bottom:* nested ADMM image after 100 global iterations.

which seemed successful for automatic parameterization in our case. Furthermore, DIP inside the reconstruction leads to better activity and shape recovery than DIP post processing. Finally, the nested ADMM can be seen as a stable way to go from the initialization image (BSREM here) to ADMMLim without penalty, and thus may present low positive bias in the cold region.

Some hyperparameters are still important to tune for the nested ADMM, such as the penalty strength ρ , and DIP learning rate and optimizer which influence the denoised DIP image. Eventually, selecting an appropriate number of iterations is necessary. Real data from a liver phantom and patients will then be used for clinical evaluation.

V. ACKNOWLEDGMENTS

This work has been partly funded by the NEXT Junior Talent project TRAC through the French “Programme d’Investissement Avenir”.

REFERENCES

- [1] S. Ahn and J. A. Fessler, “Globally convergent image reconstruction for emission tomography using relaxed ordered subsets algorithms,” *IEEE transactions on medical imaging*, vol. 22, no. 5, pp. 613–626, 2003.
- [2] S. Ahn, S. G. Ross, E. Asma, J. Miao, X. Jin, L. Cheng, S. D. Wollenweber, and R. M. Manjeshwar, “Quantitative comparison of osem and penalized likelihood image reconstruction using relative difference penalties for clinical pet,” *Physics in Medicine & Biology*, vol. 60, no. 15, p. 5733, 2015.

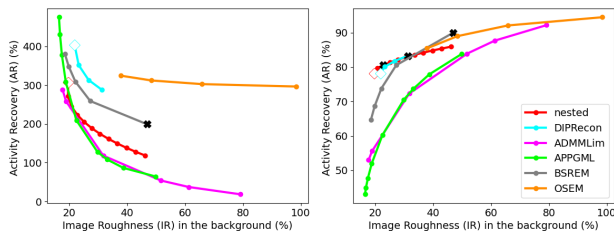


Fig. 4: Trade-off curves for 100 replicates in cold region (*left*) and hot region (*right*) for the proposed algorithm and DIPRecon (both manually tuned, default settings), ADMMLim at convergence and APPGML 15 iterations 28 subsets, both with varying penalty strength (MRF quadratic penalty), OSEM 36 iterations and 28 subsets with varying 2D FWHM Gaussian filtering, BSREM 30 iterations and 28 subsets with varying penalty strength (RDP penalty). White squares correspond to the BSREM image denoised by DIP used in DIPRecon and the proposed method. Images corresponding to black crosses are shown in Fig. 2 and Fig. 3.

- [3] K. Gong, C. Catana, J. Qi, and Q. Li, "Pet image reconstruction using deep image prior," *IEEE transactions on medical imaging*, vol. 38, no. 7, pp. 1655–1665, 2019.
- [4] H. M. Hudson and R. S. Larkin, "Accelerated image reconstruction using ordered subsets of projection data," *IEEE transactions on medical imaging*, vol. 13, no. 4, pp. 601–609, 1994.
- [5] H. Lim, Y. K. Dewaraja, and J. A. Fessler, "A pet reconstruction formulation that enforces non-negativity in projection space for bias reduction in y-90 imaging," *Physics in Medicine & Biology*, vol. 63, no. 3, p. 035042, 2018.
- [6] T. Merlin, S. Stute, D. Benoit, J. Bert, T. Carlier, C. Comtat, M. Filipovic, F. Lamare, and D. Visvikis, "Castor: a generic data organization and processing code framework for multi-modal and multi-dimensional tomographic reconstruction," *Physics in Medicine & Biology*, vol. 63, no. 18, p. 185005, 2018.
- [7] M. Millardet, S. Moussaoui, J. Idier, D. Mateus, M. Conti, C. Bailly, S. Stute, and T. Carlier, "A multiobjective comparative analysis of reconstruction algorithms in the context of low-statistics 90 y-pet imaging," *IEEE Transactions on Radiation and Plasma Medical Sciences*, vol. 6, no. 6, pp. 629–640, 2021.
- [8] J. Nuyts, D. Beque, P. Dupont, and L. Mortelmans, "A concave prior penalizing relative differences for maximum-a-posteriori reconstruction in emission tomography," *IEEE Transactions on nuclear science*, vol. 49, no. 1, pp. 56–60, 2002.
- [9] S. Stute, C. Tauber, C. Leroy, M. Bottlaender, V. Brulon, and C. Comtat, "Analytical simulations of dynamic pet scans with realistic count rates properties," in *2015 IEEE Nuclear Science Symposium and Medical Imaging Conference (NSS/MIC)*. IEEE, 2015, pp. 1–3.
- [10] D. Ulyanov, A. Vedaldi, and V. Lempitsky, "Deep image prior," in *Proceedings of the IEEE conference on computer vision and pattern recognition*, 2018, pp. 9446–9454.
- [11] H. Wang, T. Li, Z. Zhuang, T. Chen, H. Liang, and J. Sun, "Early stopping for deep image prior," *arXiv preprint arXiv:2112.06074*, 2021.
- [12] B. Wohlberg, "Admm penalty parameter selection by residual balancing," *arXiv preprint arXiv:1704.06209*, 2017.